Approximate analytical expressions of apertured broadband beams in the far field*

Lu Shi-Zhuan(陆世专)[a)b)†], You Kai-Ming(游开明)[b)], Chen Lie-Zun(陈列尊)[b)], and Wang You-Wen(王友文)[b)]

[a)] *National Laboratory of Solid State Microstructures and Department of Physics, Nanjing University, Nanjing* 210093, *China*

[b)] *Department of Physics and Electronic Information Science, Hengyang Normal University, Hengyang* 421008, *China*

(Received 24 May 2010; revised manuscript received 16 November 2010)

The approximate analytical expressions of the apertured broadband beams in the far field with Gaussian and Laguerre–Gaussian spatial modes are presented. For the radially polarized Laguerre–Gaussian beam, the result reveals that the electromagnetic field in the far field is transverse magnetic. The influences of bandwidth (Γ) and truncation parameter (C_0) on the transverse intensity distribution of the Gaussian beam and on the energy flux distribution of radially polarized Laguerre–Gaussian beam are analysed.

Keywords: broadband beams, Laguerre–Gaussian beam, apertured

PACS: 42.25.Fx, 42.60.Jf, 42.30.Kq **DOI:** 10.1088/1674-1056/20/3/034202

1. Introduction

A radially polarized beam focused by a high-numerical-aperture lens can yield a strong longitudinal component oriented along the lens axis[1] and a sharp focusing spot with its size significantly smaller than that of the linearly polarized light.[2,3] A radially polarized beam symmetrically illuminating an aperture leads to a smaller point spread function than other polarized beams.[4,5] Many efforts have been made to study radially polarized beams.[6−14] Most of these have focused on the propagation of the monochromatic light field in free space. In practice, however, due to the existence of aperture and bandwidth effects, the diffraction of ultrashort pulses[15−21] and the propagation of broadband beams in an apertured optical system[22,23] have received considerable attention. Diffraction-induced pulse transformation of pulses with a spatial Gaussian profile has also been studied.[15−18] Many interesting effects, such as pulse front curvature, pulse broadening and spectral changes have been revealed. The results presented by Peng *et al.*[22,23] showed the smoothing effect in the near field and the narrowing effect in the far field. Due to the lack of closed-form analytical expressions for the propagated field, most of the previous work has focused on numerical simulations within a paraxial approximation.

The main aim here is to explore non-paraxial propagation of a broadband radially polarized Laguerre–Gaussian beam diffracted by a circular aperture. The influence of bandwidth on spatial transverse distribution of energy flux is also analysed. The rest of the present paper is organized as follows. In Section 2, we describe the general theory for non-paraxial propagation of pulse beams. By the use of the method of stationary phase in integral, the far field behaviours of beams with spatial Gaussian and Laguerre–Gaussian modes are presented in Section 3. Finally, a summary is given in Section 4.

2. General theoretical

Assuming that there exists a spatial and temporal optical field in a certain plane $z = 0$ as a source, the radiated field $\boldsymbol{E}(x, y, x, t)$ beyond the source ($z > 0$) is governed by the wave equation

$$\left(\nabla^2 - \frac{1}{c^2}\frac{\partial^2}{\partial t^2}\right)\boldsymbol{E}(x, y, z, t) = 0, \qquad (1)$$

where c is the light speed in free space and ∇^2 is the Laplacian. Performing a time-domain Fourier trans-

*Project supported by the Doctorial Start-up Fund of Hengyang Normal University, China (Grant No. 09B06), and the Natural Science Foundation of Hunan Province, China (Grant No. 08jj3001).

†Corresponding author. E-mail: shizhuanlu@gmail.com

© 2011 Chinese Physical Society and IOP Publishing Ltd

form on both sides of Eq. (1) yields the Helmholtz equation in the frequency domain

$$\left(\nabla^2 + \frac{\omega^2}{c^2}\right)\widetilde{\boldsymbol{E}}(x,y,z,\omega) = 0. \tag{2}$$

The source $\widetilde{\boldsymbol{E}}(x_0,y_0,0,\omega)$ located at $z=0$ can be factorized into a function of frequency $\widetilde{f}(\omega)$ and a function of position $\widetilde{\boldsymbol{U}}_\omega(x_0,y_0,0)$. Monochromatic disturbances with different frequencies have the same transversal profile $\widetilde{\boldsymbol{U}}_\omega(x_0,y_0,0)$. All points of the source possess the same temporal function $f(t)$

$$f(t) = \frac{1}{\sqrt{2\pi}}\int_{-\infty}^{\infty}\widetilde{f}(\omega)\exp(-\mathrm{i}\omega t)\,\mathrm{d}\omega. \tag{3}$$

Correspondingly, the position function with a single frequency ω is determined by

$$\left(\nabla^2 + \frac{\omega^2}{c^2}\right)\widetilde{\boldsymbol{U}}_\omega(x,y,z) = 0. \tag{4}$$

Thus, the radiated field $\boldsymbol{E}(x,y,z,t)$ can be written in terms of $\widetilde{f}(\omega)\widetilde{\boldsymbol{U}}_\omega(x,y,z)$ as

$$\begin{aligned}&\boldsymbol{E}(x,y,z,t)\\ &= \frac{1}{\sqrt{2\pi}}\int_{-\infty}^{\infty}\widetilde{f}(\omega)\widetilde{\boldsymbol{U}}_\omega(x,y,z)\exp(-\mathrm{i}\omega t)\,\mathrm{d}\omega.\end{aligned} \tag{5}$$

To obtain an expression of the radiated field in the time-domain, we need to solve Eq. (4). The solution of Eq. (4) can be expressed as

$$\begin{aligned}&\widetilde{\boldsymbol{U}}_\omega(x,y,z)\\ &= \int_{-\infty}^{\infty}\int_{-\infty}^{\infty}\boldsymbol{u}_\omega(p,q,z)\exp[\mathrm{i}k(px+qy)]\,\mathrm{d}p\mathrm{d}q,\end{aligned} \tag{6}$$

where $\boldsymbol{u}_\omega(p,q,z)$ is spatial-frequency spectrum of $\widetilde{\boldsymbol{U}}_\omega(x,y,z)$ in a certain plane z; p/λ and q/λ are the spatial frequencies in the x and the y directions (λ is the wavelength and $k=2\pi/\lambda$), and $\boldsymbol{u}_\omega(p,q,z) = \boldsymbol{u}_\omega(p,q,0)\exp(\mathrm{i}k\gamma z)$ with $\gamma = \sqrt{1-p^2-q^2}$. The components of $\boldsymbol{u}_\omega(p,q,0)$ in the x and the y directions can be given by the Fourier transform of the source field as

$$\begin{aligned}u_{\omega x}(p,q,0) &= \lambda^{-2}\int_{-\infty}^{\infty}\int_{-\infty}^{\infty}\widetilde{U}_{\omega x}(x_0,y_0,0)\\ &\quad\times\exp[-\mathrm{i}k(px_0+qy_0)]\,\mathrm{d}x_0\,\mathrm{d}y_0,\end{aligned} \tag{7}$$

$$\begin{aligned}u_{\omega y}(p,q,0) &= \lambda^{-2}\int_{-\infty}^{\infty}\int_{-\infty}^{\infty}\widetilde{U}_{\omega y}(x_0,y_0,0)\\ &\quad\times\exp[-\mathrm{i}k(px_0+qy_0)]\,\mathrm{d}x_0\,\mathrm{d}y_0.\end{aligned} \tag{8}$$

The longitudinal component of the angular spectrum is given by the orthogonal relation $pu_{\omega x} + qu_{\omega y} + \gamma u_{\omega z} = 0$ as

$$u_{\omega z}(p,q,0) = -[pu_{\omega x} + qu_{\omega y}]/\gamma. \tag{9}$$

3. Examples

Here we deal with two examples: one is the broadband spatial Gaussian beam and the other is the broadband radially polarized Laguerre–Gaussian beam. We assume the two sources to have a temporal Gaussian profile with (angular) frequency ω_0, which is written as

$$f(t) = \exp(-a_\mathrm{g}^2 t^2/T_\mathrm{p}^2)\cos(\omega_0 t), \tag{10}$$

where $T_\mathrm{p} = 2a_\mathrm{g}^2/(\omega_0\Gamma)$ is the pulse duration (full width at half-maximum(FWHM)), $\Gamma = \Delta\omega/\omega_0$ is the band width, $\Delta\omega$ is the spectrum width (FWHM), and $a_\mathrm{g} = 2\sqrt{\ln 2}$. Implementing the inverse Fourier transform for Eq. (10), the spectrum $\widetilde{f}(\omega)$ is expressed as[22]

$$\widetilde{f}(\omega) = \frac{a_\mathrm{g}}{\sqrt{2}\omega_0\Gamma}\exp\left[-\frac{a_\mathrm{g}^2(\omega-\omega_0)^2}{\omega_0^2\Gamma^2}\right]. \tag{11}$$

3.1. Broadband spatial Gaussian beam

We first consider the initial broadband pulse as an apertured spatial Gaussian source with its waist located in the aperture plane $z=0$, and express it as

$$E(\rho_0,0,t) = U(\rho_0,0)f(t) \tag{12}$$

with

$$U(\rho_0,0) = \exp(-\rho_0^2/w_0^2)\mathrm{circ}(\rho_0/R), \tag{13}$$

where w_0 is the waist radius of the Gaussian beam, $\rho_0 = \sqrt{x_0^2+y_0^2}$, and R is the radius of the circular aperture. The aperture function is

$$\mathrm{circ}(\rho_0/R) = \begin{cases}1, & 0\le\rho_0<R,\\ 0, & \rho_0\ge R.\end{cases} \tag{14}$$

To obtain the analytical expression of the apertured Gaussian beam in the far field, the aperture function should be expanded into an approximate sum of complex Gaussian functions

$$\mathrm{circ}(\rho_0/R) = \sum_{m=1}^{M} B_m\exp(-C_m\rho_0^2/R^2), \tag{15}$$

where the expansion coefficients B_m and C_m can be obtained by optimization computation. Wen and Breazeale[24] obtained one of the coefficient sets, containing only ten terms of coefficients ($M=10$), to match the original circ function of Eq. (14). It was shown that a good agreement between a ten-term Gaussian beam solution and the results of numerical

integration throughout the beam field was achieved, and discrepancies existed only in the extreme near field (< 0.12 times the Fresnel distance). For the practical calculation, the accuracy is high enough when the number of terms $M = 10$.

The temporal spectrum of Eq. (12) is $\widetilde{E}(\rho_0, 0, \omega) = \widetilde{U}_\omega(\rho_0, 0)\widetilde{f}(\omega)$, where $\widetilde{U}_\omega(\rho_0, 0) = U(\rho_0, 0)$. By performing Fourier transform for Eq. (13), the angular spectrum is obtained as

$$u_\omega(p, q, 0) = \frac{z_r}{\lambda} \sum_{m=1}^{M} \frac{B_m}{1 + C_m/C_0} \times \exp\left[-\frac{p^2 + q^2}{4f^2(1 + C_m/C_0)}\right], \quad (16)$$

where $C_0 = R^2/w_0^2$ is truncation parameter, $z_r = kw_0^2/2$, and $f = 1/kw_0$. Considering the scalar field only, we have ignored the longitudinal (z) angular spectrum component here. By using the method of stationary phase in integral, from Eqs. (6) and (16), the analytical expression of the monochromatic Gaussian beam (with the frequency ω) diffracted by a circular aperture in the far field is obtained as

$$\widetilde{U}_\omega(\rho, z) = -\frac{\mathrm{i}z_r z}{r^2} \mathrm{e}^{\mathrm{i}kr} \sum_{m=1}^{M} \frac{B_m}{1 + C_m/C_0} \times \exp\left[-\frac{\rho^2}{4f^2r^2(1 + C_m/C_0)}\right], \quad (17)$$

where $r = \sqrt{x^2 + y^2 + z^2}$ and $\rho = \sqrt{x^2 + y^2}$. Substituting Eqs. (11) and (17) into Eq. (5), we obtain the analytical expression of the spatial transverse field distribution of the broadband apertured Gaussian beam in the plane z in the far field as

$$E(\rho, z, t) = -\frac{\mathrm{i}za_\mathrm{g}w_0^2}{4\omega_0 \Gamma c r^2} \exp\left(-\frac{a_\mathrm{g}^2}{\Gamma^2}\right) \times \sum_{m=1}^{M} \frac{B_m Q \exp(Q^2/P)}{(1 + C_m/C_0)P^{3/2}}, \quad (18)$$

where

$$P = \frac{1}{\omega_0^2}\left[\frac{\rho^2}{4f_0^2 r^2(1 + C_m/C_0)} + \frac{a_\mathrm{g}^2}{\Gamma^2}\right], \quad (19)$$

$$Q = \frac{1}{\omega_0}\left[\frac{a_\mathrm{g}^2}{\Gamma^2} - \frac{\mathrm{i}\omega_0}{2}\left(t - \frac{r}{c}\right)\right], \quad (20)$$

and $f_0 = c/w_0\omega_0 = 1/k_0w_0$.

Now, we analyse the influence of bandwidth on the spatial transverse intensity distribution of beam in the far field. The intensity is normalized by the maximum of $|E(\rho, z, t)|^2$. Figure 1 shows the normalized intensity distributions of Gaussian beams with different bandwidths and truncation parameters. The reference plane is at $z = 10000\lambda_0$ and $t = z/c$. The others parameters are $w_0 = 10\lambda_0$, with $\lambda_0 = 800$ nm. In Figs. 1(a) and 1(b), we take truncation parameter to be $C_0 = 4$ (in this case, the diffraction effect is in fact negligible) and $C_0 = 0.25$, respectively. The circles denote the numerical simulation results obtained from the direct numeric integrating of Eq. (5) combined with Eqs. (6), (11) and (16). Obviously, the analytical results are in good agreement with the numerical simulations. From Fig. 1, we find that the transverse intensity distribution in the far field is narrowed as the bandwidth increases. Comparing Figs. 1(a) and 1(b), one can see that the bandwidth narrowing effect becomes more significant due to the diffraction effect caused by the existence of the aperture.

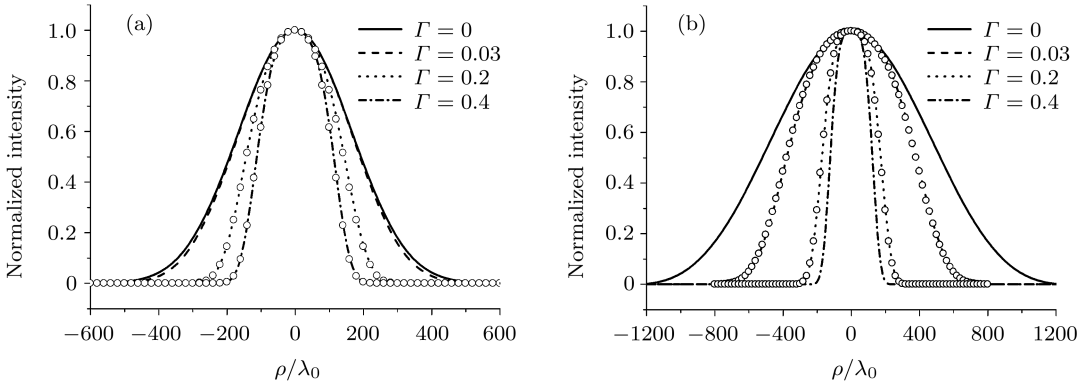


Fig. 1. Normalized transverse intensity distributions of Gaussian beams with different bandwidths in the far field. Reference plane: $z = 10000\lambda_0$ and $t = z/c$. In panel (a) $C_0 = 4$; in panel (b) $C_0 = 0.25$. Circles denote numerical results.

3.2. Broadband radially polarized Laguerre–Gaussian beam

The radially polarized beam behind the aperture can be written as

$$\boldsymbol{E}_{n1}(x_0, y_0, 0, t) = \boldsymbol{U}_{n1}(x_0, y_0, 0) f(t), \tag{21}$$

with

$$\begin{aligned}&\boldsymbol{U}_{n1}(x_0, y_0, 0)\\ &= U_{n1x}(x_0, y_0, 0)\widehat{\boldsymbol{e}}_x + U_{n1y}(x_0, y_0, 0)\widehat{\boldsymbol{e}}_y,\end{aligned} \tag{22}$$

where $\widehat{\boldsymbol{e}}_x$ and $\widehat{\boldsymbol{e}}_y$ are the unit vectors in the x and the y directions, and the corresponding components $U_{n1x}(x_0, y_0, 0)$ and $U_{n1y}(x_0, y_0, 0)$ can be written as

$$\begin{aligned}&U_{n1x}(x_0, y_0, 0)\\ &= \frac{E_0 x_0}{w_0} L_n^1\left(\frac{2\rho_0^2}{w_0^2}\right)\exp\left(-\frac{\rho_0^2}{w_0^2}\right)\mathrm{circ}\left(\frac{\rho_0}{R}\right),\end{aligned} \tag{23}$$

$$\begin{aligned}&U_{n1y}(x_0, y_0, 0)\\ &= \frac{E_0 y_0}{w_0} L_n^1\left(\frac{2\rho_0^2}{w_0^2}\right)\exp\left(-\frac{\rho_0^2}{w_0^2}\right)\mathrm{circ}\left(\frac{\rho_0}{R}\right).\end{aligned} \tag{24}$$

Here, E_0 is an arbitrary amplitude constant and $L_n^1(.)$ is the generalized Laguerre polynomial with the radial mode number n and the angular mode number 1. Performing the Fourier transformation of Eqs. (23) and (24), the x and the y components of the vector angular spectrum are obtained as

$$u_{n1x}(p, q, 0) = Cp\sum_{m=1}^{M}\frac{B_m(1 - C_m/C_0)^n}{(1 + C_m/C_0)^{2+n}}\exp\left[-\frac{p^2+q^2}{4f^2(1 + C_m/C_0)}\right]L_n^1\left[\frac{p^2+q^2}{2f^2(1 - C_m^2/C_0^2)}\right], \tag{25}$$

$$u_{n1y}(p, q, 0) = Cq\sum_{m=1}^{M}\frac{B_m(1 - C_m/C_0)^n}{(1 + C_m/C_0)^{2+n}}\exp\left[-\frac{p^2+q^2}{4f^2(1 + C_m/C_0)}\right]L_n^1\left[\frac{p^2+q^2}{2f^2(1 - C_m^2/C_0^2)}\right], \tag{26}$$

where $C = (-1)^{n+1}\mathrm{i}E_0/8\pi f^3$. From Eq. (9), u_{n1z} can be written as

$$u_{n1z}(p, q, 0) = -\frac{C(p^2+q^2)}{\gamma}\sum_{m=1}^{M}\frac{B_m(1 - C_m/C_0)^n}{(1 + C_m/C_0)^{2+n}}\exp\left[-\frac{p^2+q^2}{4f^2(1 + C_m/C_0)}\right]L_n^1\left[\frac{p^2+q^2}{2f^2(1 - C_m^2/C_0^2)}\right]. \tag{27}$$

By using the vector angular spectrum method, the propagating electric field of the monochromatic radially polarized beam can be obtained as

$$\widetilde{\boldsymbol{U}}_{\omega n1}(x, y, z) = \iint_{-\infty}^{\infty}\{u_{n1x}(p, q, 0)\widehat{\boldsymbol{e}}_x + u_{n1y}(p, q, 0)\widehat{\boldsymbol{e}}_y + u_{n1z}(p, q, 0)\widehat{\boldsymbol{e}}_z\}\exp(\mathrm{i}kN)\,\mathrm{d}p\mathrm{d}q, \tag{28}$$

where $N = px + qy + \gamma z$. From Eqs. (25)–(28), one can obtain

$$\begin{aligned}\widetilde{\boldsymbol{U}}_{\omega n1}(x, y, z) = &-\frac{\mathrm{i}\lambda C}{r^3}[zx\widehat{\boldsymbol{e}}_x + zy\widehat{\boldsymbol{e}}_y - (x^2+y^2)\widehat{\boldsymbol{e}}_z]\,\mathrm{e}^{\mathrm{i}kr}\sum_{m=1}^{M}\frac{B_m(1 - C_m/C_0)^n}{(1 + C_m/C_0)^{2+n}}\\ &\times\exp\left[-\frac{x^2+y^2}{4f^2r^2(1 + C_m/C_0)}\right]L_n^1\left[\frac{x^2+y^2}{2f^2r^2(1 - (C_m/C_0)^2)}\right].\end{aligned} \tag{29}$$

Since $L_n^1(x)$ can be expanded into $L_n^1(x) = \sum_{l=0}^{n}(-x)^l(n+1)!/[(l+1)!(n-l)!(l)!]$, from Eqs. (5), (11) and (29), we can obtain

$$\begin{aligned}\boldsymbol{E}_{n1}(x, y, z, t) = &D[zx\widehat{\boldsymbol{e}}_x + zy\widehat{\boldsymbol{e}}_y - (x^2+y^2)\widehat{\boldsymbol{e}}_z]\exp\left(-\frac{a_{\mathrm{g}}^2}{\Gamma^2}\right)\sum_{l=0}^{n}\sum_{m=1}^{M}\left[-\frac{(x^2+y^2)w_0^2}{2c^2r^2(1 - C_m^2/C_0^2)}\right]^l\\ &\times\frac{(n+1)!}{(l+1)!(n-l)!l!}\frac{B_m(1 - C_m/C_0)^n}{(1 + C_m/C_0)^{2+n}}\int_{-\infty}^{\infty}\omega^{2l+2}\exp(-E\omega^2 + 2F\omega)\,\mathrm{d}\omega,\end{aligned} \tag{30}$$

where

$$D = (-1)^{n+1}\frac{a_{\mathrm{g}}E_0w_0^3}{8\sqrt{\pi}r^3c^2\omega_0\Gamma}, \tag{31}$$

$$E = \frac{(x^2+y^2)w_0^2}{4c^2r^2(1 + C_m/C_0)} + \frac{a_{\mathrm{g}}^2}{\omega_0^2\Gamma^2}, \tag{32}$$

$$F = \frac{a_{\rm g}^2}{\omega_0 \Gamma^2} + \frac{\rm i}{2}(r/c - t). \tag{33}$$

Integrating Eq. (30), the analytical expression of the electric field can be written as

$$\begin{aligned}\boldsymbol{E}_{n1}(x,y,z,t) = {} & D[zx\widehat{\boldsymbol{e}}_x + zy\widehat{\boldsymbol{e}}_y - (x^2+y^2)\widehat{\boldsymbol{e}}_z]\exp\left(-\frac{a_{\rm g}^2}{\Gamma^2}\right)\sum_{l=0}^{n}\sum_{m=1}^{M}\left[-\frac{(x^2+y^2)w_0^2}{2c^2r^2(1-C_m^2/C_0^2)}\right]^l \\ & \times \frac{(n+1)!}{(l+1)!(n-l)!l!}\frac{B_m(1-C_m/C_0)^n}{(1+C_m/C_0)^{2+n}}\frac{\sqrt{\pi}}{2^{2l+1}E^{3/2}}\frac{\partial^{2l+1}}{\partial F^{2l+1}}[F\exp(F^2/E)].\end{aligned} \tag{34}$$

In a similar way, we can write magnetic field as

$$\begin{aligned}\boldsymbol{H}_{n1}(x,y,z,t) = {} & Dr(-y\widehat{\boldsymbol{e}}_x + x\widehat{\boldsymbol{e}}_y)\sqrt{\frac{\varepsilon_0}{\mu_0}}\exp\left(-\frac{a_{\rm g}^2}{\Gamma^2}\right)\sum_{l=0}^{n}\sum_{m=1}^{M}\left[-\frac{(x^2+y^2)w_0^2}{2c^2r^2(1-C_m^2/C_0^2)}\right]^l \\ & \times \frac{(n+1)!}{(l+1)!(n-l)!l!}\frac{B_m(1-C_m/C_0)^n}{(1+C_m/C_0)^{2+n}}\frac{\sqrt{\pi}}{2^{2l+1}E^{3/2}}\frac{\partial^{2l+1}}{\partial F^{2l+1}}[F\exp(F^2/E)].\end{aligned} \tag{35}$$

Equations (34) and (35) give the approximate analytical expressions for the electric and the magnetic fields of the apertured broadband radially polarized Laguerre–Gaussian beams in the far field. The equations could provide a powerful and convenient tool for investigating the propagation properties of a pulsed radially polarized Laguerre–Gaussian beam diffracted by a circular aperture. It can be seen from Eq. (35) that there exists no longitudinal (z) magnetic field component, implying that this particular electromagnetic field is transverse magnetic.

The energy flux distribution in the far field of apertured radially polarized Laguerre–Gaussian beam is given by the z component of the Poynting vector as

$$\begin{aligned}S_{n1z} = {} & D^2zr(x^2+y^2)\sqrt{\frac{\varepsilon_0}{\mu_0}}\exp\left(-\frac{2a_{\rm g}^2}{\Gamma^2}\right)\left|\sum_{l=0}^{n}\sum_{m=1}^{M}\left[-\frac{(x^2+y^2)w_0^2}{2c^2r^2(1-C_m^2/C_0^2)}\right]^l\right. \\ & \left.\times\frac{(n+1)!}{(l+1)!(n-l)!l!}\frac{B_m(1-C_m/C_0)^n}{(1+C_m/C_0)^{2+n}}\frac{\sqrt{\pi}}{2^{2l+1}E^{3/2}}\frac{\partial^{2l+1}}{\partial F^{2l+1}}[F\exp(F^2/E)]\right|^2.\end{aligned} \tag{36}$$

We define the normalized energy flux as S_{n1z} divided by the maximum of S_{n1z}. For the sake of intuition, the influence of bandwidth on the normalized energy flux distribution of beam in the plane $z = 10000\lambda_0$ is depicted in Fig. 2. The parameters used for plots in Fig. 2 are $w_0 = 10\lambda_0$ and $\lambda_0 = 800$ nm. In Fig. 2(a) $C_0 = 1$ and the radial mode number $n = 0$, and in Fig. 2(b) $C_0 = 3.61$ and radial mode number $n = 1$. It can also be seen that the simulation results are in accordance with the analytical results. From Fig. 2(a), we can find that the peak is closer to the centre and the peak width decreases as bandwidth increases. The outermost diffraction fringe is suppressed by the broadband beam. Figure 2(b) shows that as bandwidth increases, the inner peak is enhanced while the outer peak is suppressed, in particular, the inner and the outer peaks are both close to the centre.

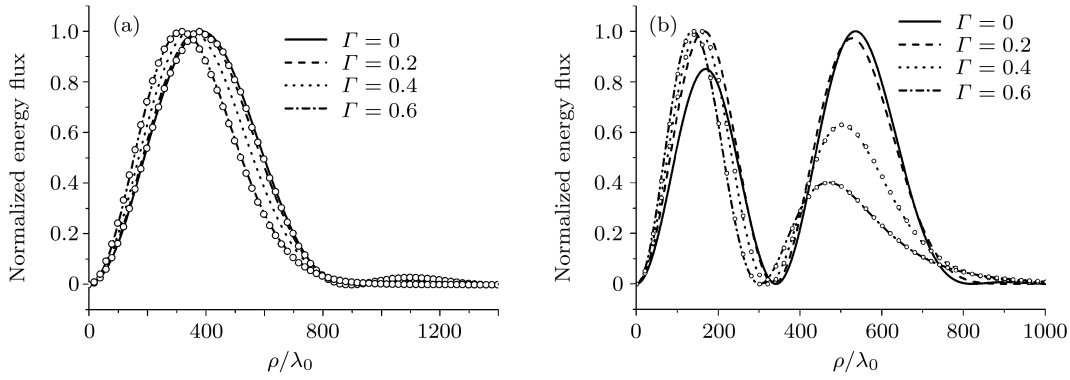


Fig. 2. Normalized energy flux distributions of Laguerre–Gaussian beams with different bandwidths in the far field, with reference plane $z = 10000\lambda_0$ and $t = z/c$. In panel (a) $C_0 = 1$ and the radial mode number $n = 0$; in panel (b) $C_0 = 3.61$ and the radial mode number $n = 1$. Circles denote numerical results.

4. Conclusion

Approximate analytical expressions of an apertured broadband beam with Gaussian and Laguerre–Gaussian modes in the far field have been presented. The stationary-phase method is used to obtain Eqs. (17) and (29), which are valid under the condition $kr = k(x^2 + y^2 + z^2)^{1/2} \to \infty$. This condition is satisfied in the far field regime. The effect of bandwidth on the light intensity distribution of apertured Gaussian beam in the far field is analysed. We find that the width of transverse intensity distribution decreases as bandwidth increases and the narrowing effect of the transverse intensity distribution is present in the far field. We have also analysed the influence of bandwidth on energy flux distributions of radially polarized Laguerre–Gaussian beam with zero-order and first-order radial modes. The results show that the bandwidth effect causes the peaks of energy flux distributions to be close to the centre.

References

[1] Biss D P and Brown T G 2001 *Opt. Express* **9** 490
[2] Quabis S, Dorn R, Eberler M, Glockl O and Leuchs G 2001 *Appl. Phys.* B **72** 109
[3] Dorn R, Quabis S and Leuchs G 2003 *Phys. Rev. Lett.* **91** 233901
[4] Cooper I J, Roy M and Sheppard C J R 2005 *Opt. Express* **13** 1066
[5] Lu D Q, Hu W, Qian L J and Fan D Y 2009 *Acta. Phys. Sin.* **58** 1655 (in Chinese)
[6] Tovar A A 1998 *J. Opt. Soc. Am.* A **15** 2705
[7] Shoham A, Vander R and Lipson S G 2006 *Opt. Lett.* **31** 3405
[8] Kuga T, Torii Y, Shiokawa N, Hirano T, Shimizu Y and Sasada H 1997 *Phys. Rev. Lett.* **78** 4713
[9] Niziev A G and Nesterov A V 1999 *J. Phys.* D **32** 1455
[10] Sick B, Hecht B and Novotny L 2000 *Phys. Rev. Lett.* **85** 4482
[11] Salamin Y I 2006 *Opt. Lett.* **31** 2619
[12] Deng D M 2006 *J. Opt. Soc. Am.* B **23** 1228
[13] Deng D M and Guo Q 2007 *Opt. Lett.* **32** 2711
[14] Yan S H and Yao B L 2007 *Opt. Lett.* **32** 3367
[15] Christov I P 1985 *Opt. Commun.* **53** 364
[16] Ziolkowski R W and Judkins J B 1992 *J. Opt. Soc. Am.* A **9** 2021
[17] Kaplan A E 1998 *J. Opt. Soc. Am.* B **15** 951
[18] Porras M A 2002 *Phys. Rev.* E **65** 026606
[19] Porras M A 1998 *Phys. Rev.* E **58** 1086
[20] Brabec T and Krausz F 2000 *Rev. Mod. Phys.* **72** 545
[21] Chen B S and Pu J X 2010 *Chin. Phys.* B **19** 074202
[22] Peng R W, Ye Y X, Tang Z X and Fan D Y 2005 *J. Opt. Soc. Am.* A **22** 1903
[23] Peng R W, Tang Z X, Ye Y X, Wen S C and Fan D Y 2007 *Opt. & Laser Technol.* **39** 900
[24] Wen J J and Breazeale M A 1990 *Computational Acoustics* **2** 181